

**Comprehensively understanding the distinct properties of
crystal structure, phase transition and dielectrics in
[M(crown)_n]ReO₄ (M⁺ = Na⁺, K⁺, NH₄⁺; crown = 15-crown-5,
18-crown-6; n = 1 or 2)**

Guo-Jun Yuan^{*ab} Xue-Wei Pan^b Yan Gao^b You-Fang Jiang^c Li Li^a Xiao-Ming Ren^{*b}

^a Department of Chemistry, Nanjing Xiaozhuang University, Nanjing 211171, P. R. China

^b State Key Laboratory of Materials-Oriented Chemical Engineering and College of Chemistry and molecular of Engineering, Nanjing Tech University, Nanjing 211816, P. R. China

^c Jingde Ziyang School of Anhui Province, XuanCheng 242600, P. R. China

Tel.: +86 25 58139476

Email: ahchljygj@163.com (GJY); xmren@njtech.edu.cn (XMR)

Contents

Fig. S1: Comparison of simulated and experimental Powder X-ray diffraction profiles for **1–3**.

Fig. S2: Packing diagram (a) viewed along the *b*- and (b) *c*-axes, respectively, for **2** at 296 K, where the green dash lines represent the weaker H-bonding interactions between the O atoms of anion and the H atoms of crown-ether ring.

Fig. S3: (a) An asymmetric unit with non-hydrogen atom labeling (the thermal ellipsoids are drawn at 30% probability level), (b) one dimensional (1D) supramolecular chain, (c) illustration of H-bonds, (d-f) Packing diagram viewed along the *a*-, *b*- and *c*-axes, respectively, for **2** at 108 K.

Fig. S4: Packing diagram viewed along (a) the *a*- and *b*-axes for **3** at 296 K, where the green dash lines represent the weaker H-bonding interactions between the O atoms of anion and the H atoms of crown-ether ring.

Fig. S5: (a) Dimer structure for **3** at 108 K; (b–d) Packing diagram viewed along the *a*-, *b*- and *c*-axes for **3** at 108 K.

Fig. S6: (a) Plots of ϵ' vs. temperature in the 153–470 K range for **1**; (b) Plots of ϵ' vs. temperature in the 153–450 K range for **2**; (c) Plots of ϵ' vs. temperature in the 153–450 K range for **3**.

Fig. S7: Plot of $\ln(1/\tau)$ vs. $1000/T$ in the 153–470 K range for **1**, where the solid squares represent the experimental data, and the red line is reproduced by fitted parameters.

Fig. S8: Variable-temperature PXRD patterns of **3** at the selected temperatures, corresponding to three different phases, respectively.

Table S1: Selected bond lengths / Å for **1** at 296 K

Table S2: Selected bond lengths / Å for **2** at 296 K

Table S3: Selected bond lengths / Å for **2** at 108 K

Table S4: Selected bond lengths / Å for **3** at 296 K

Table S5: Selected bond lengths / Å for **3** at 108 K

Table S6: The value of ΔH , ΔS and N at the selected temperature for **1–3**

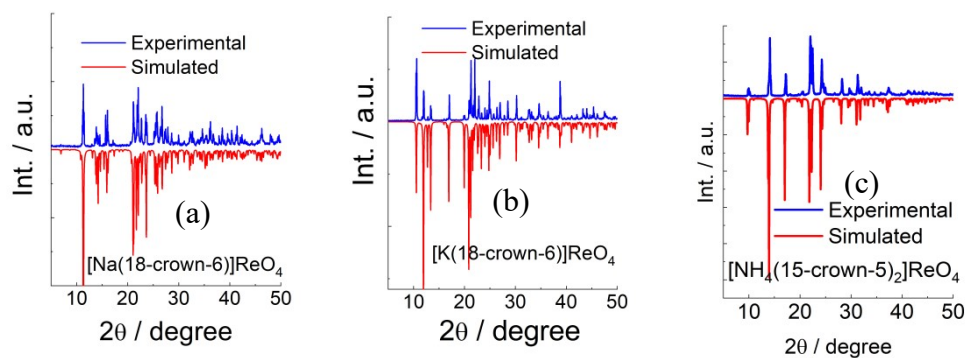


Fig. S1: Comparison of simulated and experimental Powder X-ray diffraction profiles for 1–3.

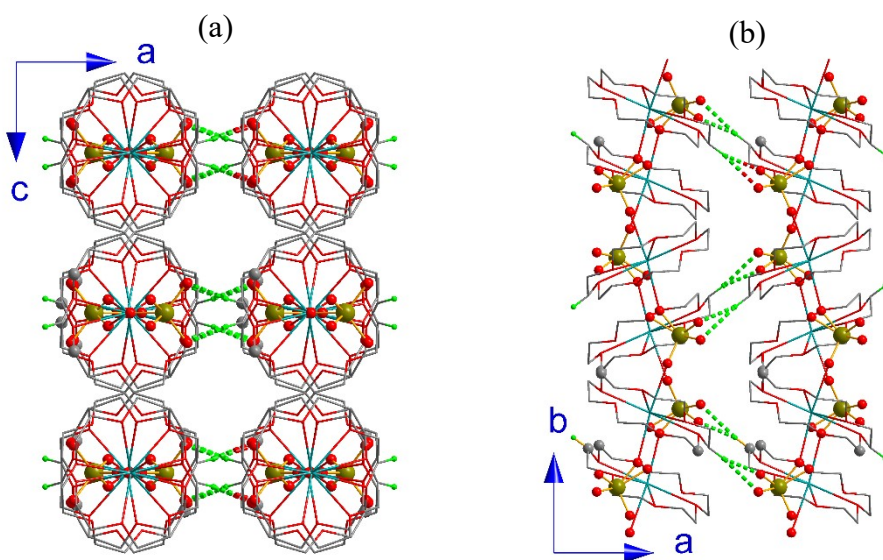


Fig. S2: Packing diagram (a) viewed along the b - and (b) c -axes, respectively, for **2** at 296 K, where the green dash lines represent the weaker H-bonding interactions between the O atoms of anion and the H atoms of crown-ether ring.

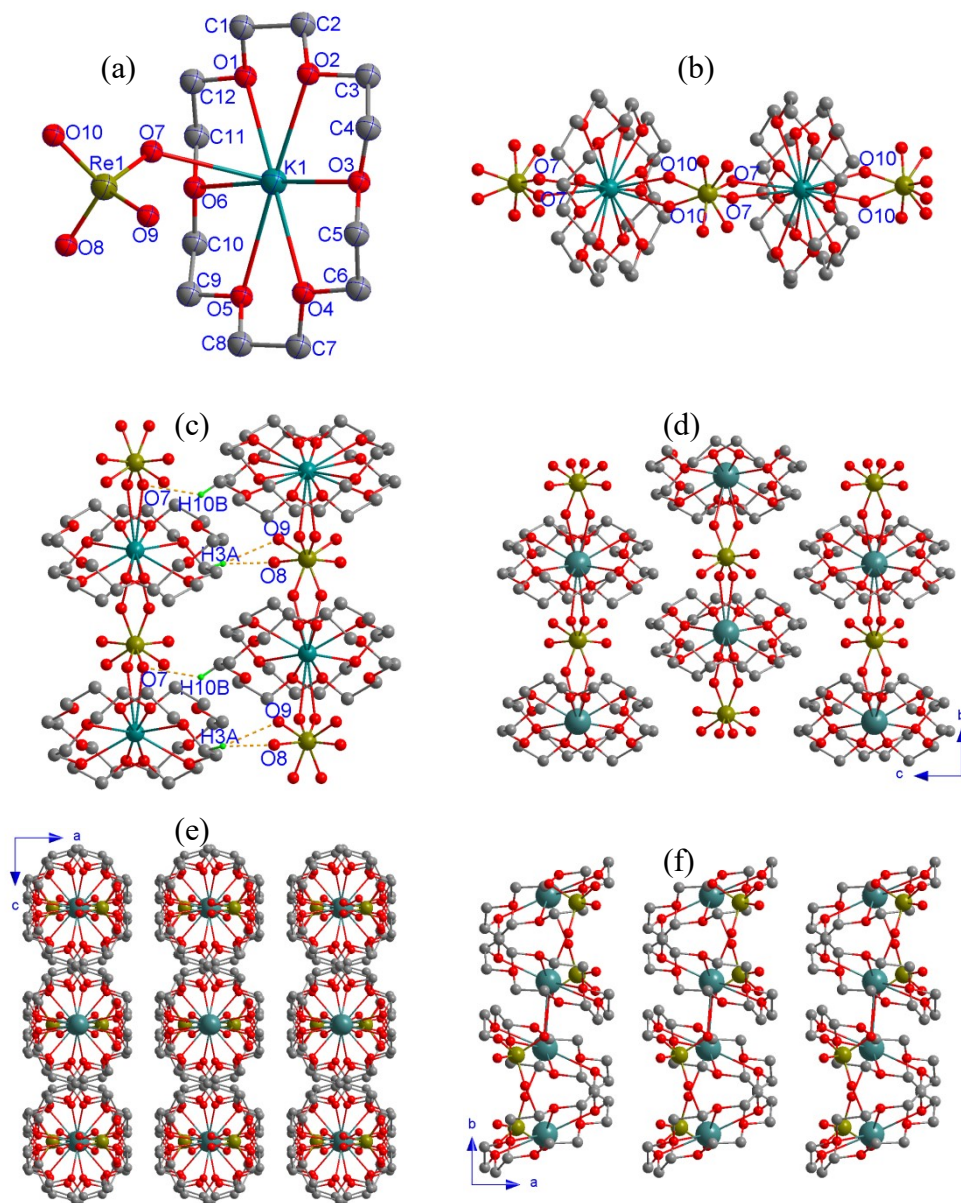


Fig. S3: (a) An asymmetric unit with non-hydrogen atom labeling (the thermal ellipsoids are drawn at 30% probability level), (b) one dimensional (1D) supramolecular chain, (c) illustration of H-bonds, (d-f) Packing diagram viewed along the *a*-, *b*- and *c*-axes, respectively, for **2** at 108 K.

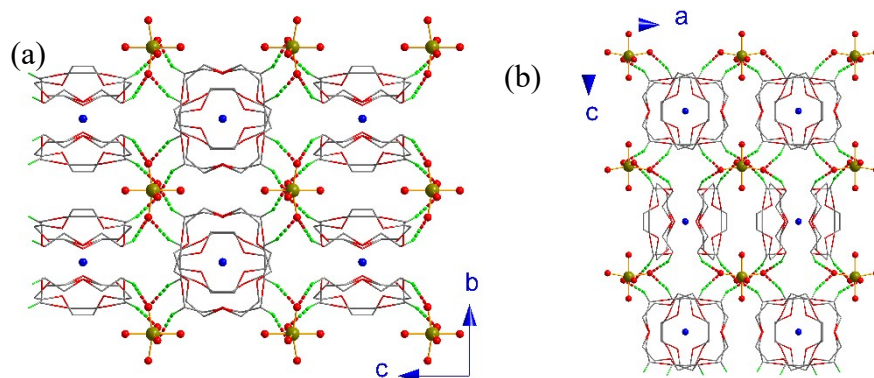


Fig. S4: Packing diagram viewed along (a) the *a*- and *b*-axes for **3** at 296 K, where the green dash lines represent the weaker H-bonding interactions between the O atoms of anion and the H atoms of crown-ether ring.

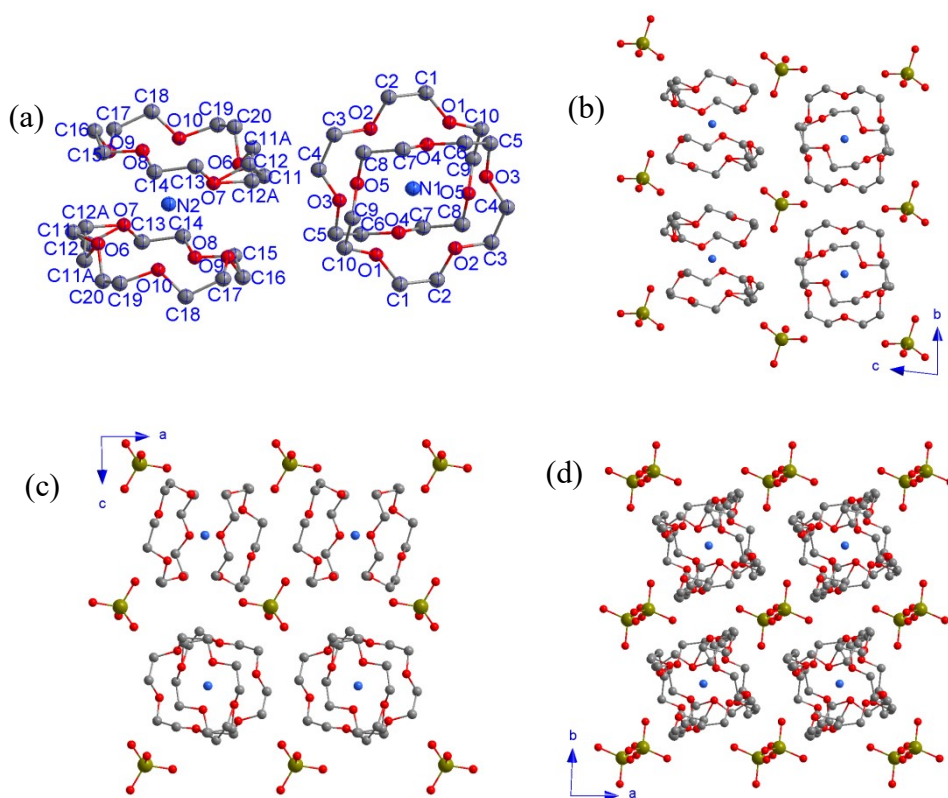


Fig. S5: (a) Dimer structure for **3** at 108 K; (b–d) Packing diagram viewed along the *a*-, *b*- and *c*-axes for **3** at 108 K.

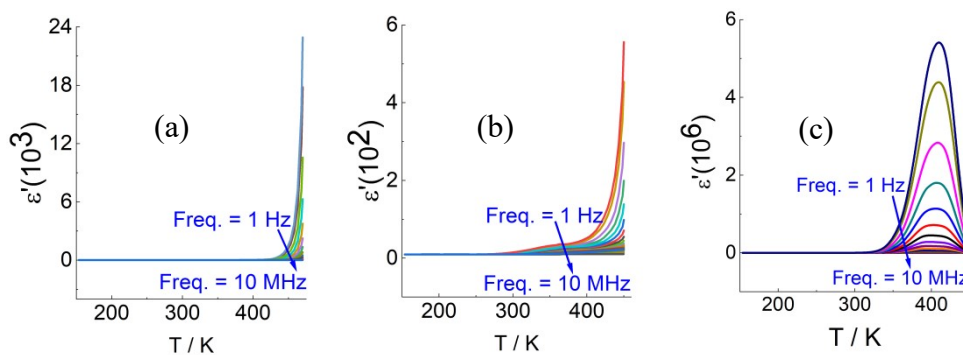


Fig. S6: (a) Plots of ϵ' vs. temperature in the 153–470 K range for **1**; (b) Plots of ϵ' vs. temperature in the 153–450 K range for **2**; (c) Plots of ϵ' vs. temperature in the 153–450 K range for **3**.

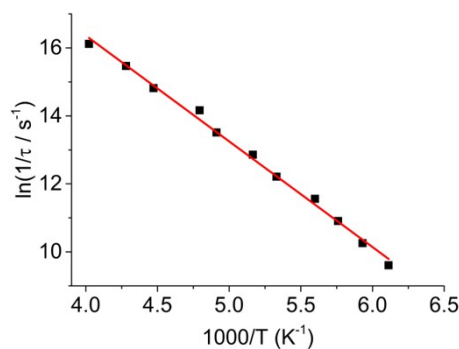


Fig. S7: Plot of $\ln(1/\tau)$ vs. $1000/T$ in the 153–470 K range for **1**, where the solid squares represent the experimental data, and the red line is reproduced by fitted parameters.

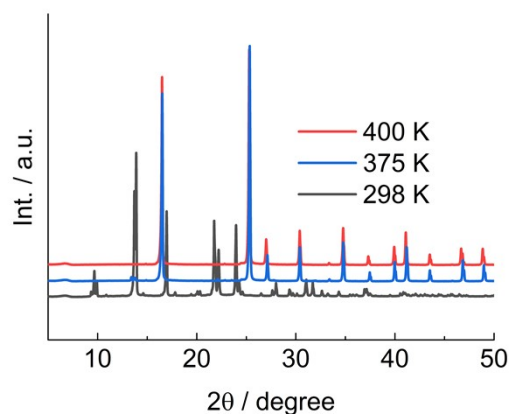


Fig. S8: Variable-temperature PXRD patterns of **3** at the selected temperatures, corresponding to three different phases, respectively.

Table S1: Selected bond lengths / Å for **1** at 296 K

Bond	Bond lengths	Bond	Bond lengths
Na(1)-O(1)	2.8483(8)	Na(2)-O(7)	2.3878(5)
Na(1)-O(2)	2.5845(5)	Na(1)-O(10)	2.4254(5)
Na(1)-O(3)	2.7014(5)	Re(1)-O(7)	1.7355(5)
Na(2)-O(4)	2.7641(6)	Re(1)-O(8)	1.7219(6)
Na(2)-O(5)	2.7433(6)	Re(1)-O(9)	1.7121(6)
Na(2)-O(6)	2.6452(3)	Re(1)-O(10)	1.7170(5)
Na(2)-O(6)A	2.6496(3)		

Table S2: Selected bond lengths / Å for **2** at 296 K

Bond	Bond lengths	Bond	Bond lengths
K(1)-O(1)	2.8449(2)	K(1)-O(7)	2.7739(2)
K(1)-O(2)	2.9396(2)	Re(1)-O(7)	1.7143(2)
K(1)-O(3)	2.9109(2)	Re(1)-O(8)	1.7180(3)
K(1)-O(4)	2.8030(2)	Re(1)-O(8)A	1.7517(3)
K(1)-O(5)	2.6593(2)	Re(1)-O(9)	1.8378(5)
K(1)-O(6)	2.7184(2)	Re(1)-O(9)A	1.6597(5)

Table S3: Selected bond lengths / Å for **2** at 108 K

Bond	Bond lengths	Bond	Bond lengths
K(1)-O(1)	2.8257(2)	K(1)-O(7)	2.8311(1)
K(1)-O(2)	2.7240(1)	K(1)-O(10)	2.7302(1)
K(1)-O(3)	2.6905(1)	Re(1)-O(7)	1.7459(1)
K(1)-O(4)	2.8316(1)	Re(1)-O(8)	1.7171(1)
K(1)-O(5)	2.9405(1)	Re(1)-O(9)	1.749(1)
K(1)-O(6)	2.8920(1)	Re(1)-O(10)	1.7330(1)

Table S4: Selected bond lengths / Å for **3** at 296 K

Bond	Bond lengths	Bond	Bond lengths
N(1)-O(1)	3.1916(2)	N(1)-O(3)	3.1208(6)
N(1)-O(1)A	2.8702(2)	N(1)-O(3)A	2.9766(6)
N(1)-O(2)	3.1313(2)	Re(1)-O(4)	1.7566(5)
N(1)-O(2)A	2.7989(3)	Re(1)-O(5)	1.7761(3)

Table S5: Selected bond lengths / Å for **3** at 108 K

Bond	Bond lengths	Bond	Bond lengths
N(1)-O(1)	2.9320(5)	N(2)-O(8)	3.1172(5)
N(1)-O(2)	3.0052(5)	N(2)-O(9)	2.8666(5)
N(1)-O(3)	2.8485(5)	N(2)-O(10)	2.9858(5)
N(1)-O(4)	3.0295(5)	Re(1)-O(11)	1.7015(7)
N(1)-O(5)	3.0436(5)	Re(1)-O(12)	1.7142(5)
N(2)-O(6)	2.9146(6)	Re(1)-O(13)	1.7270(5)
N(2)-O(7)	3.0156(6)	Re(1)-O(14)	1.7077(6)

Table S6: The value of ΔH , ΔS and N at the selected temperature for **1–3**

	1	2	3	3
Temp. (K)	436	360	289	352
ΔH (kJ mol ⁻¹)	16.11	21.02	4.28	3.38
ΔS (J K ⁻¹ mol ⁻¹)	36.95	58.38	14.80	9.61
N	85.1	1120.9	5.9	3.2